JACS
JOURNAL OF THE AMERICAN CHEMICAL SOCIETY

ARTICLE

pubs.acs.org/JACS

Single Molecule Tracking Analysis Reveals That the Surface Mobility of Amyloid Oligomers Is Driven by Their Conformational Structure

Martino Calamai* and Francesco S. Pavone

University of Florence, European Laboratory for Nonlinear Spectroscopy (LENS), Sesto Fiorentino, Florence 50019, Italy

Supporting Information

ABSTRACT: Several models have been proposed to explain the cytotoxicity of Aβ oligomers. The structural polymorphism of the oligomers can account for the various toxic effects observed. By combining the use of conformation-specific antibodies and single particle tracking techniques, we have investigated the mobility of individual Aβ1−42 oligomers on the plasma membrane of living cells. Distinct structural types of Aβ1−42 oligomers were labeled with two different conformation-specific antibodies. While both types of oligomers showed a heterogeneous dynamic behavior, their overall mobility was found to be significantly different. Conversely, we discovered that other amyloid oligomers sharing a similar conformation but composed of different peptides (amylin and prion Sup35NM) display dynamic behaviors comparable to those found for Aβ1−42 oligomers. This study provides evidence for a link between the quaternary structure and the membrane mobility of proteins, revealing that structurally analogous supramolecular assemblies diffuse similarly in cells.

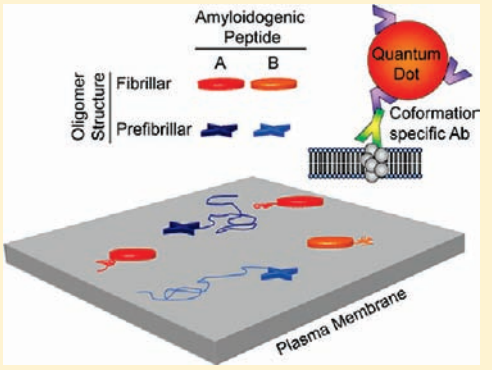

INTRODUCTION

Alzheimer's disease (AD) is a highly debilitating neurodegenerative pathology characterized by the extracellular deposition in the brain of fibrillar aggregates consisting predominantly of the Aβ peptide.[1] The presence of fibrils is the hallmark not only of AD, but also of other diseases, such as type II diabetes mellitus. In the latter, however, the fibrils are composed of the peptide amylin (also known as islet amyloid polypeptide, IAPP) and are accumulated specifically in the pancreatic islets.[2] Amyloid fibrils, although formed by different peptides and proteins, commonly display a peculiar structural arrangement of β-sheets disposed perpendicularly to the main fibril axis.[3,4] An increasing body of evidence points at oligomeric species (the term oligomer is used here to describe any nonmonomeric form of an amyloidogenic protein that is soluble in aqueous solutions and remains in solution after high-speed centrifugation) that accumulate during fibril formation as crucial factor of toxicity.[5]

In particular, several models have been proposed to describe the mechanisms of neurotoxicity of Aβ oligomers, including the alteration of extracellular and intracellular membrane permeability and the interaction with various receptors.[6−8] However, regardless of the model considered, the cytotoxic effect inevitably involves an initial interaction of the oligomers with the plasma membrane. Although this interaction has been the object of intense investigation, one point that still needs to be properly addressed is the dynamic behavior of the oligomers once bound to the membrane.

The variety of cytotoxic effects ascribed to the oligomers and associated to the complexity of AD may be attributable to their polymorphism.[7,9−13] Several morphologically and structurally different forms of similarly sized Aβ oligomers have been characterized. A big step forward within this context has been the production of antibodies able to recognize distinct aggregate conformations.[14,15]

Here, we question the influence of quaternary structure on the dynamic behavior of different oligomeric assemblies by coupling a single molecule approach with the use of conformation-specific antibodies.

EXPERIMENTAL SECTION

Cell Culture. Human SH-SY5Y neuroblastoma cells were obtained from A.TCC (Manassas, VA) and cultured in 1:1 Dulbecco's modified Eagle's medium (DMEM)/F-12 supplemented with 10% fetal bovine serum (FBS) and 1.0% antibiotics. Cell cultures were maintained in a 5.0% CO_2 humidified atmosphere at 37 °C and grown until 80% confluence. Cells were used for a maximum of 20 passages. H-END cells were kindly provided by Prof. F. Bussolino (University of Turin, Italy) and cultured in DMEM containing 10% FBS, 3.0 mM glutamine, 100 units/mL penicillin, and 100 μg/mL streptomycin in a 5.0% CO_2 humidified atmosphere at 37 °C.

Oligomers Preparation and Cells Treatment. Aβ1−42 (A9810) and amylin (D2162) were purchased from Sigma. N-terminal conjugated Hilyte Fluor 488 Aβ1−42 (60479) and TAMRA-Aβ1−42 (60476) were purchased from Anaspec. Amylin, Aβ1−42, Aβ1−42hi488, or TAMRA-Aβ1−42 peptides were initially incubated in hexafluoroisopropanol (HFIP) at room temperature for 1 h. The HFIP was evaporated under a gentle stream of N_2. Dried peptide aliquots were dissolved in

Received: January 31, 2011
Published: July 01, 2011

anhydrous DMSO to a final concentration of 5.0 mM, diluted into ice-cold phenol red-free F12 medium to 100 μM and incubated at 4 °C for 24 h (4 h or 1 month where specified). Alternatively, Aβ1−42 stock solutions (2 mM) were prepared by dissolving the lyophilized peptide in 100 mM NaOH followed by water bath sonication for 30 s. The oligomerization reaction was initiated by diluting the stock solution in PBS to a final concentration of 45 μM, pH 7.4, and incubated at room temperature for 24 h.[16] Sup35NM samples were a gift from Prof. M. Bucciantini (University of Florence, Italy) and Prof. R. Melki (CNRS, Gif-sur-Yvette, France). Sup35NM was expressed and purified under denaturing conditions as previously described[17] and stored at −80 °C in 8 M urea, 20 mM sodium phosphate, pH 7.5, 150 mM NaCl, and 5 mM β-mercaptoethanol. To achieve assembly, Sup35NM was dialyzed against the assembly buffer (20 mM Tris-HCl, pH 8.0, 200 mM NaCl, 5% glycerol, 5 mM β-mercaptoethanol, and 10 mM $MgCl_2$). After dialysis, the protein samples were incubated at 4 °C for one month at a concentration of 90 μM. Aβ1−42, amylin, and Sup35NM samples were centrifuged for 15 min at 14 000*g* and the supernatant fraction was transferred to the cell medium to a final concentration of 10 μM monomer equivalent. Dynamic light scattering measurements confirm that the size of the oligomers after centrifugation is <10 nm. Images of large aggregates and fibrils present before centrifugation are shown in Supporting Information.

Giant Unilamellar Vesicles (GUVs) Preparation. 1-Palmitoyl-2-oleoyl-*sn*-glycero-3-phosphocholine (POPC)/0.0005% lissamine-rhodamine phosphatidylethanolamine (Rh-PE) GUVs (Avanti lipids) were a gift of Dott. D. Berti (University of Florence, Italy). GUVs were formed in a 60 mM sucrose solution through electroformation.

Single Particle Imaging. Quantum dots (QDs) labeling and live imaging has been extensively described.[18] Briefly, living cells or GUVs were incubated at 37 °C with amyloid oligomers (20 min), then washed and incubated with primary (20 min) and secondary (10 min) antibodies in phenol red-free Leibovitz's L-15 medium 10% FBS, followed by QDs (1 min) in QD binding buffer. GUVs were centrifuged 5 min at 4000*g* and the supernatant discarded after each step. Rabbit polyclonal OC (1:10 000 dilution) and I11 (1:2000 dilution), mouse anti-Aβ monoclonal (β-Amyloid DE2B4, Santa Cruz Biotechnology, Inc., 1:100 dilution), mouse anti-amylin monoclonal (Amylin R10/99, Santa Cruz Biotechnology, Inc., 1:50 dilution), and rabbit polyclonal anti-Sup35 (gift from Prof. R. Melki, 1:5000 dilution) antibodies were used as primary antibodies. Biotinylated anti-mouse or anti-rabbit Fab antibodies (Jackson Laboratories and Abcam, respectively) were used as secondary antibodies at 1:400 dilution. Streptavidin-coated QDs (Invitrogen) emitting at 655 nm were used at 1:10 000 dilution. Alternatively, anti-mouse F(ab')$_2$-QDs 655 (Invitrogen) were used. No labeling was observed when cells were incubated in the absence of oligomers. Cells were monitored with a custom-made wide-field epifluorescence or TIRF microscope equipped with an oil-immersion objective (Nikon Plan Apo TIRF 60×/1.45), an argon ion laser (Reliant 150 Select, excitation line 488 nm), and a heating chamber. Dichroic FF499-Di01-25 × 36 and emission FF01-655/15-25 (for QDs) or FF01-530/43-25 (for Aβ1−42hi488) filters (Semrock) were used. A total of 250 or 100 consecutive frames were acquired with an integration time of 80 or 300 ms, respectively, with an intensified charge-coupled device camera PI-Max (Roper Scientific) using WinView (PI Acton, Roper Scientific). Recording sessions did not last more than 30 min.

Single Particle Tracking. Tracking of single QDs, which were identified by their fluorescence intermittence, was performed with MATLAB (MathWorks, Natick, MA) using a homemade routine that accounts for blinking in the fluorescence signal.[18−20] In brief, the method consists of two main steps, applied successively to each frame of the sequence. First, fluorescent spots are detected by cross-correlating the image with a Gaussian model of the microscope Point Spread Function. A least-squares Gaussian fit is applied (around the local maximum above a threshold) to determine the center of each spot with a spatial precision of 10−20 nm (depending on the signal-to-noise ratio). Second, QD trajectories are assembled automatically by linking, from frame to frame, the centers of fluorescent spots likely from the same QD. The association criterion is based on the assumption of free Brownian diffusion and takes into account short blinking events. After completion of the process, a manual association step is performed, in which QD trajectories of maximal length are assembled from smaller fragments separated by longer blinking events that were not taken into account by the automatic linking procedure. Aβ1−42hi488 clusters and TAMRA-Aβ1−42 oligomers were tracked using the Particle Tracker[21] plug-in developed on ImageJ software.

Quantitative Analysis of Diffusion Coefficient. Analyses of mean square displacement (MSD) and initial diffusion coefficient (D) are reported in the literature.[18,20] Briefly, physical parameters can be extracted from each trajectory ($x(t)$,y(t)) by computing the MSD,[22] determined from the following formula:

$$\mathrm{MSD}(\mathrm{d}t) = \frac{1}{N-n}\sum_{i=1}^{N-n}\left[(x_{(i+n)} - x_i)^2 + (y_{(i+n)} - y_i)^2\right]$$

where x_i and y_i are the coordinates of a particle on frame i, dt is the time between two successive frames, N the total number of frames of the trajectory and nd$t$ the time interval over which the displacement is averaged. This function enables the analysis of the lateral dynamics on short (initial diffusion coefficient) and long (types of motion) time scales. Different types of motion can be distinguished from the time dependence of the MSD.[22] The initial diffusion coefficient (D) is determined by fitting the initial 2−5 points of the MSD against time plot with $\mathrm{MSD}(t) = 4D_{2-5}t + b$. The cumulative probability C(d) of D defines the probability that D is inferior to d. The median D value is found at $C = 0.5$. We compared cumulative probability distributions and median instead of mean values because D values were spread over 4 orders of magnitude.

Quantitative Analysis of Velocity. The velocity v of actively transported particles was determined by calculating the mean displacement (MD) during the acquisition time interval dt:

$$v = MD\ \mathrm{d}t^{-1}$$

Alternatively, similar v values were obtained by fitting the MSD against time plot with the equation for directed motion[22] $\mathrm{MSD}(t) = 4Dt + (vt)^2$.

Internalization Test. The cells were incubated with Aβ1−42 oligomers and labeled as described above in Single Particle Imaging. Low pH stripping was then performed 30 min after the final labeling step with QDs by incubating cells at 2 °C in 0.2 M acetic acid, 0.5 M NaCl, pH 2.2, for 7 min.

Statistical Analysis. Data are expressed as mean ± standard error of the mean (SEM). Comparisons between the different groups were performed by Student t test or ANOVA followed by Tukey's *post hoc* test. A p-value <0.05 was considered statistically significant.

RESULTS

Distinct Surface Mobility of Prefibrillar and Fibrillar Aβ1−42 Oligomers. Preformed Aβ1−42 oligomers were incubated with SH-SY5Y neuroblastoma cells (a cell line commonly used to study the cytotoxic effects of amyloid oligomers[14]) for 20 min and subsequently labeled with primary antibodies, secondary biotin-Fab fragments, and streptavidin-coated quantum dots (QDs). We took advantage of structure-specific primary antibodies to immunochemically label distinct conformations of Aβ1−42 oligomers concomitantly present in the same sample, avoiding therefore the necessity to obtain samples

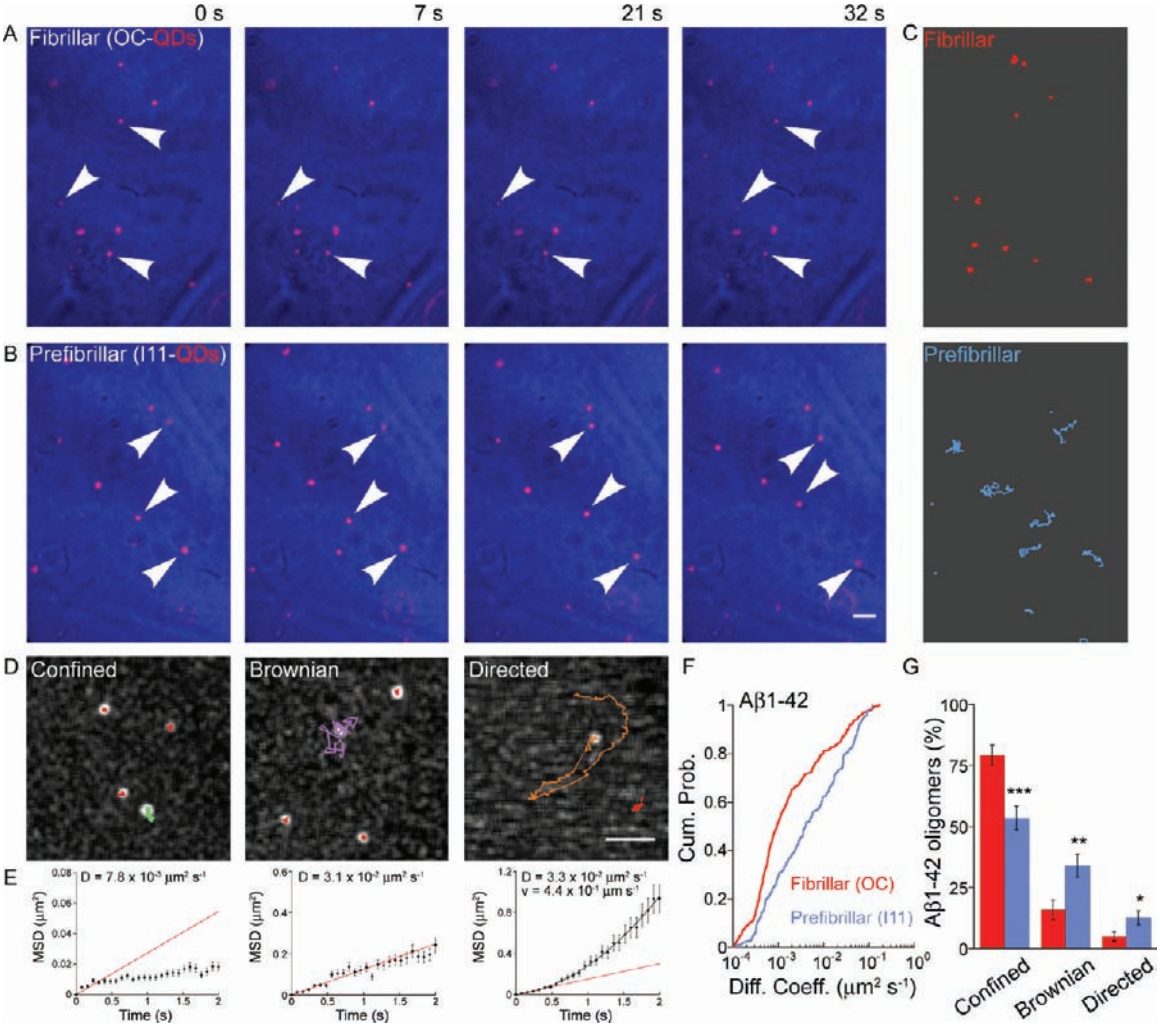

Figure 1. Heterogeneous dynamic behavior of Aβ1−42 oligomers in human neuroblastoma cells. (A and B) Live imaging of membrane bound fibrillar and prefibrillar Aβ1−42 oligomers labeled with the conformation-specific antibodies OC (A) and I11 (B), Fab-biotin secondary antibodies and streptavidin QDs. The bright-field image of the cell is in false color only for chromatic contrast purposes. Cells had been incubated for 20 min with preformed oligomers. The trajectories of the oligomers interpolated from (A) and (B) are reported in (C). (D) Examples of trajectories showing distinct types of motion of Aβ1−42 oligomers. Scale bars, 2 μm. (E) MSD plot of the green, purple, and orange trajectories analyzed in (D), respectively. The instantaneous diffusion coefficient D was calculated from the linear fit of the first initial points of the MSD plot. (F) Cumulative probability distributions of diffusion coefficients from fibrillar (red) and prefibrillar (blue) oligomer trajectories. (G) Quantification of oligomers per cell classified according to the type of motion inferred from the MSD plot of each oligomer. Mean ± SEM, $n > 10$ cells. Student t test, $p \leq 10^{-3}$ (***), 10^{-2} (**), and 5×10^{-2} (*).

of oligomers with a single morphology and high purity. We used two different types of conformation-specific antibodies directed against amyloid oligomers with prefibrillar (I11) and fibrillar (OC) morphologies. The OC and I11 antibodies have been previously produced in response to immunization with Aβ1−42 fibrils and amylin prefibrillar oligomer mimics,[15] respectively. Both antibodies do not recognize the amyloidogenic monomers. Despite the name, the prefibrillar oligomers recognized by I11 do not necessarily represent species on the pathway to fibril formation, but rather represent an alternate assembly pathway.[16] On the other hand, the fibrillar oligomers may correspond to small pieces of fibrils or fibril nuclei. Both fibrillar and prefibrillar oligomers have been detected in human brains affected by AD.[14,15,23] The sizes of Aβ1−42 oligomers recognized by OC and I11 overlap broadly (Figure S1). OC and I11 recognize oligomers in the range of 8 kDa (dimers) up to 250 and 100 kDa,[15] respectively. In agreement with previous observations,[15] the fibrillar population is the most represented (Figure S1) under the main aggregation conditions followed here (ice-cold F12, see Experimental Section). Nonetheless, the higher sensitivity of single particle tracking (SPT) technique allowed us to detect also prefibrillar species. Only individual oligomers that remained bound to the plasma membrane after incubation and that were labeled with a single QD (as suggested by blinking) were considered for the analysis.

Within the time scale of the recordings (~30 s), both prefibrillar and fibrillar oligomers bound to QDs exhibited most of the typical dynamic behaviors that have been generally observed for membrane proteins (Figure 1A−D and Movies S1−S5 in the Supporting Information). The trajectories of the oligomers were sorted according to their individual mean square displacement (MSD) against time plot curvature and the oligomers were classified into three types, depending on whether they mainly followed a confined, Brownian or directed motion

Table 1. Diffusion Coefficients of Different Amyloid Oligomers on the Plasma Membrane of SH-SY5Y Neuroblastoma Cells[a]

oligomers (primary antibody)	D_{median} ($\mu m^2\ s^{-1}$)	Δ_{max}[b]	p[c]
Aβ1−42 (OC)	9.4×10^{-4}		
Aβ1−42 (I11)	4.0×10^{-3}	2.7×10^{-1}	$<10^{-3}$
Aβ1−42hi488 (OC)	6.5×10^{-4}		
Aβ1−42hi488 (I11)	1.3×10^{-3}	3.6×10^{-1}	$<10^{-3}$
Amylin (OC)	9.7×10^{-4}		
Amylin (I11)	2.1×10^{-3}	3.5×10^{-1}	$<10^{-3}$
Prion Sup35NM (OC)	7.4×10^{-4}		
Prion Sup35NM (I11)	1.2×10^{-3}	2.4×10^{-1}	$<10^{-3}$
Aβ1−42 (anti-Aβ1−42)	6.1×10^{-4}		
Amylin (anti-Amylin)	5.2×10^{-4}	1.5×10^{-1}	1.6×10^{-2}
Prion Sup35NM (anti-Sup35)	9.1×10^{-4}	1.0×10^{-1}	1.2×10^{-1}

[a] Cells were incubated with distinct oligomers solutions. [b] Maximum difference in the cumulative probability of the diffusion coefficient (D) of distinct amyloid oligomers. The type of oligomer of reference to calculate the difference for each group is highlighted in bold characters. [c] Kolmogorov−Smirnov test p-value calculated using Δ_{max} as statistic. For each condition, $100 < n < 400$.

(Figure 1D,E). Aβ1−42 oligomers that appear to undergo a directed motion are likely to be part of an intracellular vesicle (see Supporting Information Figures S2 and S3). A few oligomers (~ 2%) showed also changes from one type of motion to another (Figure S4).

To explore to which extent a different conformation could affect the lateral diffusion of the oligomers, we compared the diffusion coefficients (D) of prefibrillar and fibrillar oligomers (Figure 1F and Table 1). We found significantly different D value distributions. The median D of prefibrillar oligomers was 4 times higher than for fibrillar oligomers. We did not observe significant changes in the diffusive behavior of fibrillar and prefibrillar oligomers preaggregated for different times (4 h, 24 h, and 1 month, see Table S1), although the amount of labeled oligomers was lower for aggregation times shorter or longer than 24 h. In addition, the diffusive trend did not change under alternative aggregation conditions that enriched the population of prefibrillar oligomers[15] (NaOH/PBS, see Experimental Section, and Table S1).

The distribution of oligomers classified according to their type of motion was found to be significantly different (Figure 1G). A much higher amount of fibrillar oligomers (75%) appeared to be confined with respect to prefibrillar ones (50%).

These results show that Aβ1−42 oligomers display multiple types of motions, although they appear to be predominantly confined, and demonstrate that their diffusive features are strictly dependent on their structural conformation.

The Diffusive Behavior of Amyloid Oligomers Is Independent of Their Primary Sequence. In addition to Aβ1−42, various amyloidogenic peptides and proteins can form oligomers that interact with the plasma membrane and induce cell death. The conformation-specific antibodies OC and I11 (used here to discriminate between prefibrillar and fibrillar Aβ1−42 oligomers) can also recognize structurally similar motifs of aggregates formed by other amyloidogenic peptides.[15] For this reason, we used these antibodies to monitor the surface mobility of oligomers formed by human amylin and the isolated

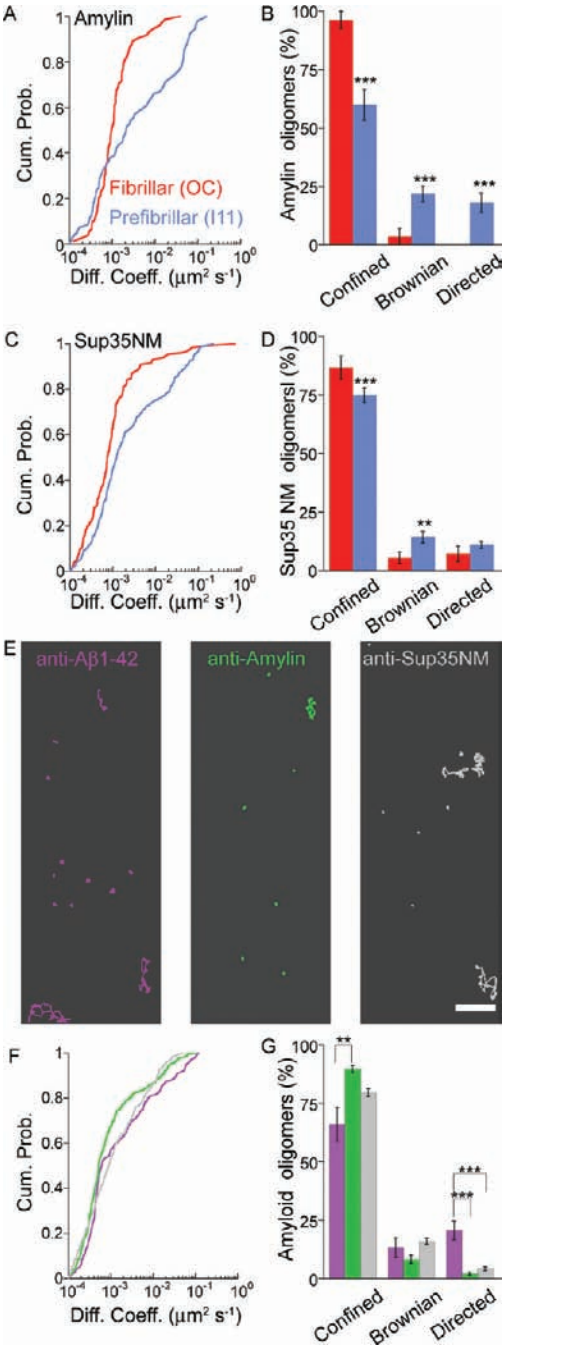

Figure 2. Structurally analogous amyloid oligomers but formed by different peptides display comparable dynamic behaviors. (A and C) Cumulative probability plots of diffusion coefficients of fibrillar (red) and prefibrillar (blue) amylin (A) and Sup35NM (C) oligomers. (B and D) Quantification of amylin (B) and Sup35NM (D) oligomers per cell classified according to their type of motion. Mean ± SEM, $n >$ 10 cells. Student t test, $p \leq 10^{-3}$ (***) and 10^{-2} (**). Note that in these experiments conformation-specific antibodies were used to label fibrillar and prefibrillar species. (E) Examples of trajectories of Aβ1−42, amylin, and Sup35NM oligomers labeled with sequence-specific antibodies, Fab antibodies, and QDs. Scale bar, 2 μm. (F and G) Cumulative probability plots of diffusion coefficients (F) and quantification according to the type of motion (G) of oligomers labeled with antibodies specific for Aβ1−42 (purple), amylin (green), and Sup35NM (gray). Mean ± SEM, $n >$ 10 cells. ANOVA followed by Tukey's *post hoc* test, $p \leq 10^{-3}$ (***) and 10^{-2} (**).

NM domain of the yeast prion Sup35 (Sup35NM). The interaction of amylin oligomers with the membrane is thought to be the main factor determining the death of pancreatic β-cells in type II diabetes.[2] Prion Sup35 is not associated to any disease, but it contains a highly amyloidogenic structural motif and has been used extensively as a model peptide for studying amyloid aggregation.[17,24] In the latter case, the species incubated with the cells are mostly constituted by a mixture of fragments of mature fibrils and oligomers (long fibrils as those reported in Figure S5 were not present in the samples after centrifugation). We specifically chose this particular assembly state of Sup35NM in light of recent results showing that fibril fragments with sizes comparable to those of amyloid oligomers can bind to membranes and be equally cytotoxic.[25]

Prefibrillar amylin oligomers displayed a median D value 2-fold higher than fibrillar (Figure 2A and Table 1). As found in the case of Aβ1−42 oligomers, the amount of confined fibrillar amylin oligomers (95%) was dramatically higher than prefibrillar (60%) (Figure 2B). The differences in the median D values and the distribution of Sup35NM oligomers according to the types of motion were less pronounced but still significant between prefibrillar and fibrillar species (Figure 2C,D and Table 1).

Overall, the median D values of prefibrillar or fibrillar oligomers found for Aβ1−42, amylin, and Sup35NM were comparable (Table 1). To strengthen further this result, we carried out tracking experiments using antibodies specific for each peptide, in place of those conformation-specific. The analysis of trajectories of anti-Aβ1−42, anti-amylin, and anti-Sup35NM labeled species revealed substantially equivalent dynamic behaviors (Figure 2E−G and Movie S7). The median D values of the oligomers formed by these different peptides lied in an interval between 5 and 10 $\times$ 10^{-4} μm^2 s^{-1} (Figure 2F and Table 1). Furthermore, these median D values are comparable to those found when OC antibodies were used to label the oligomers of Aβ1−42, amylin, and Sup35NM (Table 1). The fraction of anti-Aβ1−42, anti-amylin, and anti-Sup35NM labeled species diffusing randomly on the cell surface does not exceed 25%, while those confined represent the majority (>65%). The distributions of these oligomers according to their type of motion are not just quite similar between them but also to what has been found using the conformation-specific antibodies (Figure 2G). Nevertheless, the amount of confined oligomers labeled by sequence-specific antibodies appears to be lower than that found using the OC antibody. This result might be explained by considering that in theory the peptide specific antibodies could recognize both prefibrillar and fibrillar species.

The similarity between the dynamic features of Aβ1−42, amylin, and Sup35NM found using peptide specific antibodies and the conformation-specific OC antibody not only indicates that most of the oligomers bound to the membrane are effectively fibrillar in structure, but also that structurally similar amyloid oligomers formed by distinct peptides have similar membrane dynamics.

Additional Factors Affecting the Surface Mobility of Aβ1−42 Oligomers. QD labeling enables to track Aβ1−42 oligomers with high sensitivity and spatial resolution. By contrast, the size of the antibodies−QD complex could influence the mobility of the oligomers. In addition, early dynamic events, such as oligomer clustering, occurring within the dead-time required by the labeling procedure would be missed with this approach. We therefore used oligomers formed by Aβ1−42 peptides covalently linked to TAMRA dye (TAMRA-Aβ1−42) to avoid the labeling step and thus reduce the dead-time before imaging down to

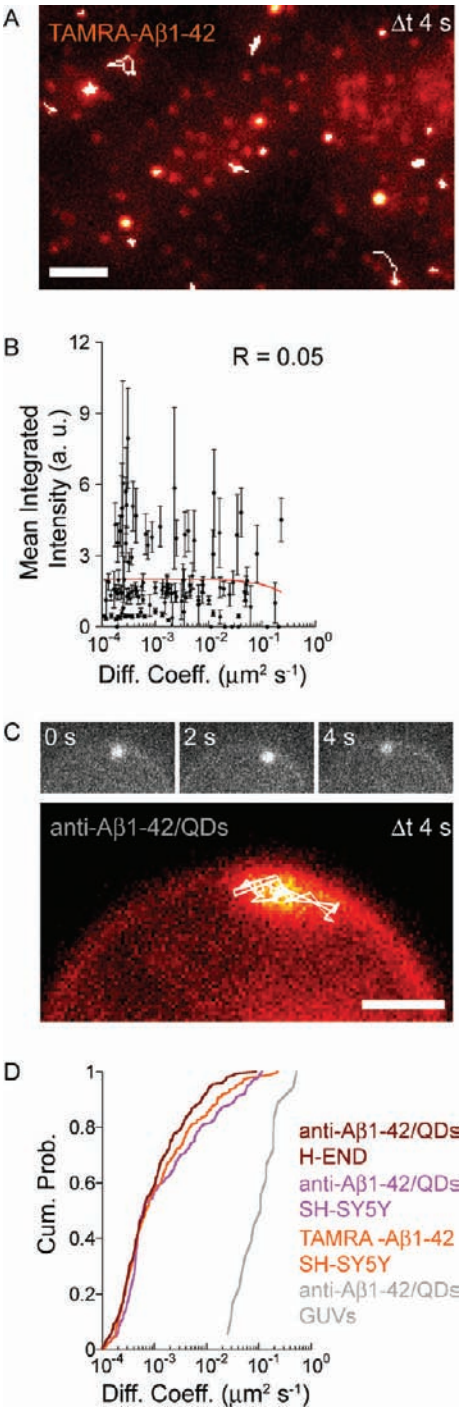

Figure 3. Factors governing the lateral diffusion of Aβ1−42 oligomers. (A) Examples of trajectories showing distinct types of motion of Aβ1−42 oligomers labeled with TAMRA superimposed over the z projection of a stack of images acquired using TIRFM. Scale bars, 2 μm. (B) The integrated intensity of individual TAMRA-Aβ1−42 oligomers averaged over time is plotted against their instantaneous diffusion coefficient. The low R value of the linear fit indicates that the data are not correlated. Error bars, SD. (C) Real-time imaging of an Aβ1−42 oligomer labeled with anti-Aβ1−42 antibody, Fab antibody and QD bound to the surface of a synthetic GUV (POPC/Rh-PE). GUVs had been incubated for 20 min with preformed oligomers. The trajectory of the oligomer is reported over the z projection of the image stack. (D) Cumulative probability distributions of diffusion coefficients from Aβ1−42 oligomers labeled with TAMRA (orange), or anti-Aβ1−42, Fabs and QDs in SH-SY5Y cells (purple), H-END cells (brown), and GUVs (gray).

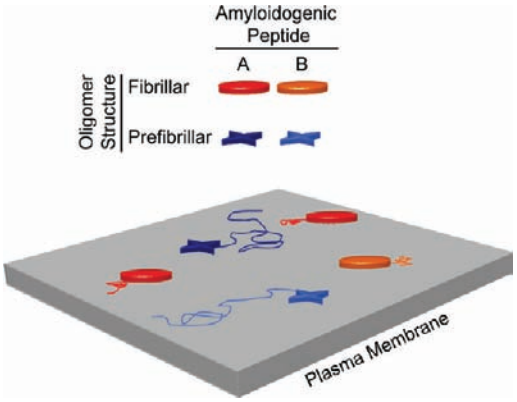

Figure 4. Schematic representation of oligomer mobility dependence on conformation. Amyloidogenic peptides can form conformationally distinct oligomers (fibrillar and prefibrillar) that display different lateral diffusion on the plasma membrane. The dynamic behavior of fibrillar or prefibrillar oligomers formed by peptides with different primary sequences (A and B) is however comparable.

5 min (minimal time of incubation with cells). A total internal reflection fluorescence microscope (TIRFM) was used to increase the signal-to-noise ratio. The TIRF setup enabled us to observe the dynamics of oligomers bound to the basal plasma membrane. The mobility displayed by TAMRA-Aβ1−42 oligomers and the distribution of their D values (Figure 3A,D, Movie S8 and Table S2) did not differ significantly from those of Aβ1−42 oligomers labeled with QDs. No significant correlation was found between the mean integrated intensity of the oligomers and their D values (Figure 3B). Since the fluorescence intensity signal of each tracked oligomer is proportional to the number of TAMRA-Aβ1−42 peptides forming it, this result suggests that size is not a major factor determining the mobility of the oligomers.

To determine whether the confined mobility of Aβ1−42 oligomers was due to interactions with specific cellular proteins, we performed SPT experiments similar to those described above but using synthetic giant unilamellar vesicles (GUVs) and murine endothelioma H-END cells instead of human neuroblastoma SH-SY5Y cells. POPC/Rh-PE GUVs were filled with a sucrose solution, subsequentely diluted in glucose to make them sink, incubated with preformed Aβ 1−42 oligomers and finally labeled with anti-Aβ1−42 and QDs. Surprisingly, the oligomers bound to the surface of the GUVs were highly mobile and technically difficult to track (Figure 3C and Movie S9). We were nevertheless able to determine D for a statistically sufficient number of oligomers. The median D value was found to be 1.1×10^{-1} μm^2 s^{-1}, approximately 2 to 3 orders of magnitude higher than in living cells (Figure 3D and Table S2). The dynamic behavior of the oligomers in H-END cells was substantially comparable to that observed in SH-SY5Y cells, although the difference between the two cumulative distributions of D resulted to be statistically significant (Figure 3D and Table S2).

These results suggest that the reduced mobility of Aβ1−42 oligomers is mainly attributable to their interaction with specific cellular structures, rather than simply to their size.

DISCUSSION

The most striking finding emerging from our experiments regards the link between structure and mobility of amyloid oligomers. Our results demonstrate that amyloid oligomers that are sharing similar structural features display a common diffusive behavior on the surface of living cells despite being formed by distinct peptides (Aβ1−42, amylin, and Sup35NM) (Figure 4). Conversely, differences in structure, even for oligomers formed by the same peptide, are reflected in significant differences in mobility (Figure 4). These results are consistent with the hypothesis of a common mechanism of cytotoxicity for all types of amyloids.[14,26] Additional specific interactions might nevertheless be involved for each type of amyloidogenic peptide (indeed, the median D values are not identical) and for each type of oligomer conformation. Furthermore, for each type of oligomer conformation, several diffusive behaviors (confined, directed, and Brownian motion) are observed. This heterogeneity of dynamics may reflect different mechanisms of toxicity.

A generic event of binding to the membrane and subsequent diffusion to more specific targets could take place. However, only a small fraction of oligomers displayed free mobility, indicating that the search for specific binding partners through lateral diffusion rarely occurs. In contrast, the low mobility of the oligomers could influence the dynamics of more mobile proteins and lipids that get in contact with them.

The reduced mobility of the oligomers could be determined by the size of the fluorescent probe or the inherent size of the oligomers. However, at the scale of nanosized probes as QDs, the movements of transmembrane proteins are not governed by the mass of the probe, but are rather dependent on the membrane viscosity, which is 100- to 1000-fold greater than that of the extracellular medium.[27] The procedure of QD-labeling has been already used to track transmembrane receptors displaying much higher D values than those observed here for amyloid oligomers.[28] Our data show that the mobility of oligomers formed by peptides covalently linked to a small dye (∼1−2 nm) is comparable to that of oligomers labeled with antibodies and QDs (>20 nm), clearly demonstrating that the size of the fluorescent probe is negligible in our measurements. Moreover, the diffusion is not dependent on the primary antibody used, since our results show that the observed diffusion properties do not change substantially when a peptide-specific rather than a conformation-specific antibody is used.

To determine to which extent the size of the oligomers could theoretically influence their diffusion, we considered the continuum hydrodynamic model proposed by Saffman and Delbrück.[29] The model describes the lateral diffusion of transmembrane proteins in a lipid bilayer as cylinders in a thin viscous sheet. This approximation is commonly used in biophysics to relate the size of membrane inclusions to their diffusion coefficients. According to this theory, the diffusion coefficient D of the cylinders is only weakly (logarithmically) dependent on their lateral radius (R). Experimental measurements of transmembrane proteins mobility in reconstituted lipid bilayers have shown that the dependence of D on size is better described by $1/R$ than $\ln(1/R)$. As proposed by Guigas et al.,[30] when a scaling $D \sim 1/R^2$ is used to calculate the diffusion of a particle with R = 10 nm the resulting D would be $\sim 10^{-1}$ μm^2 s^{-1}. This theoretical D value is exquisitely in agreement with our measurements on Aβ1−42 oligomers moving on the surface of synthetic GUVs (median $D = 1.1 \times 10^{-1}$ μm^2 s^{-1}). If we consider the cellular crowding, the theoretical D value would be decreased by an additional order of magnitude.[31] Nonetheless, the experimental median D values that we found for amyloid oligomers in cells range between 10^{-4} and 10^{-3} μm^2 s^{-1}, 2 orders of magnitude

lower than theoretically expected. D values close to 10^{-3} μm^2 s^{-1} have been measured for membrane proteins as large as the membrane flagellar basal bodies (3200 kDa).[32] By contrast, the size of Aβ1−42 oligomers studied here does not exceed 250 kDa (approximately 2−60 monomers, usually less than 10 nm in diameter). The blinking behavior often observed in the case of TAMRA-Aβ1−42 implies a relatively low number of monomers forming the oligomers bound to the membrane. All these considerations, together with the lack of correlation between the fluorescence intensity of individual TAMRA-Aβ1−42 oligomers and their diffusion coefficients, point out that, under the conditions studied here, size has only a marginal influence on the confined dynamic behavior of the oligomers. Clustering of Aβ oligomers has been proposed to explain the reduced mobility of the oligomers following binding to the membrane.[33] Under our experimental conditions, however, we did not detect any relevant event of clustering, except for those oligomers that were internalized and underwent intracellular transport (a phenomenon not observed by Renner et al.[33]).

Mobile transmembrane proteins usually display D values (measured from SPT experiments) ranging from 10^{-2} to 1 μm^2 s^{-1}, whereas for slow diffusing or less mobile proteins, the D value lies between 10^{-4} and 10^{-3} μm^2 s^{-1}. Cytoskeleton[34,35] and extracellular matrix[36] have been found to be responsible for slowing down the dynamics of transmembrane proteins. The confinement or low mobility of the oligomers, a behavior not observed in synthetic liposomes, might therefore be due to interactions with elements linked to these cellular structures. Within this context, evidence shows that amyloid deposits are associated with glycosaminoglycans, typical components of the extracellular matrix. Further research is necessary to explain the reduced mobility of the oligomers.

The results obtained here on the intimate behavior of toxic oligomers help to improve the general understanding of the basic mechanisms of amyloid diseases.

■ ASSOCIATED CONTENT

Supporting Information. Movie S1, synamic behavior of prefibrillar and fibrillar Aβ1−42 oligomers; Movie S2, example of Aβ1−42 oligomer displaying confined motion; Movie S3, example of Aβ1−42 oligomer displaying Brownian motion; Movie S4, example of Aβ1−42 oligomer displaying directed motion; Movie S5, example of Aβ1−42 oligomer switching from Brownian to confined motion; Movie S6, example of actively transported Aβ1−42hi488 oligomers; Movie S7, dynamic behavior of Aβ1−42, amylin and Sup35NM oligomers; Movie S8, Dynamic behavior of TAMRA-Aβ1−42; Movie S9, dynamic behavior of Aβ1−42 in GUVs (mpg and avi files). Figure S1, Western blot analysis of Aβ1−42 oligomers; Figure S2, internalized Aβ1−42 oligomers are actively transported in the cell; Figure S3, images of internalized QDs labeled Aβ1−42 oligomers; Figure S4, example of Aβ1−42 oligomer switching from Brownian to confined motion in human neuroblastoma cells; Figure S5, examples of amyloid species present before centrifugation; Table S1, diffusion coefficients of Aβ1−42 oligomers on the plasmamembrane of SH-SY5Y neuroblastoma cells; Table S2, diffusion coefficients of Aβ1−42 oligomers using different systems and fluorescent probes (pdf). This material is available free of charge via the Internet at http://pubs.acs.org.

■ AUTHOR INFORMATION

Corresponding Author
calamai@lens.unifi.it

Funding Sources
The work was supported by the European Union Seventh Framework Programme (FP7/2007−2013) under grant agreements no. 228334 and PIEF-GA-2009−254791.

■ ACKNOWLEDGMENT

We thank C. Glabe for providing the conformation-specific antibodies OC and I11, M. Bucciantini and R. Melki for Sup35 aggregates, D. Berti and C. Montis for GUVs, M. Capitanio for technical advice and assistance, F. Vanzi and members of the C. Dobson laboratory for critical discussions.

■ REFERENCES

(1) Hardy, J.; Selkoe, D. J. *Science* **2002**, *297* (5580), 353–6.
(2) Engel, M. F. *Chem. Phys. Lipids* **2009**, *160* (1), 1–10.
(3) Sunde, M.; Blake, C. *Adv. Protein Chem.* **1997**, *50*, 123–59.
(4) Dobson, C. M. *Nature* **2003**, *426* (6968), 884–90.
(5) Caughey, B.; Lansbury, P. T. *Annu. Rev. Neurosci.* **2003**, *26*, 267–98.
(6) LaFerla, F. M.; Green, K. N.; Oddo, S. *Nat. Rev. Neurosci.* **2007**, *8* (7), 499–509.
(7) Sakono, M.; Zako, T. *FEBS J.* **2010**, *277* (6), 1348–58.
(8) Demuro, A.; Parker, I.; Stutzmann, G. E. *J. Biol. Chem.* **2010**, *285* (17), 12463–8.
(9) Petkova, A. T.; Leapman, R. D.; Guo, Z.; Yau, W. M.; Mattson, M. P.; Tycko, R. *Science* **2005**, *307* (5707), 262–5.
(10) van der Wel, P. C.; Lewandowski, J. R.; Griffin, R. G. *J. Am. Chem. Soc.* **2007**, *129* (16), 5117–30.
(11) Madine, J.; Jack, E.; Stockley, P. G.; Radford, S. E.; Serpell, L. C.; Middleton, D. A. *J. Am. Chem. Soc.* **2008**, *130* (45), 14990–5001.
(12) Uversky, V. N. *FEBS J.* **2010**, *277* (14), 2940–53.
(13) Stefani, M. *Curr. Protein Pept. Sci.* **2010**, *11* (5), 343–54.
(14) Kayed, R.; Head, E.; Thompson, J. L.; McIntire, T. M.; Milton, S. C.; Cotman, C. W.; Glabe, C. G. *Science* **2003**, *300* (5618), 486–9.
(15) Kayed, R.; Head, E.; Sarsoza, F.; Saing, T.; Cotman, C. W.; Necula, M.; Margol, L.; Wu, J.; Breydo, L.; Thompson, J. L.; Rasool, S.; Gurlo, T.; Butler, P.; Glabe, C. G. *Mol. Neurodegener.* **2007**, *2*, 18.
(16) Necula, M.; Kayed, R.; Milton, S.; Glabe, C. G. *J. Biol. Chem.* **2007**, *282* (14), 10311–24.
(17) Krzewska, J.; Tanaka, M.; Burston, S. G.; Melki, R. *J. Biol. Chem.* **2007**, *282* (3), 1679–86.
(18) Bannai, H.; Levi, S.; Schweizer, C.; Dahan, M.; Triller, A. *Nat. Protoc.* **2006**, *1* (6), 2628–34.
(19) Bonneau, S.; Dahan, M.; Cohen, L. D. *IEEE Trans. Image Process.* **2005**, *14* (9), 1384–95.
(20) Ehrensperger, M. V.; Hanus, C.; Vannier, C.; Triller, A.; Dahan, M. *Biophys. J.* **2007**, *92* (10), 3706–18.
(21) Sbalzarini, I. F.; Koumoutsakos, P. *J. Struct. Biol.* **2005**, *151* (2), 182–95.
(22) Saxton, M. J.; Jacobson, K. *Annu. Rev. Biophys. Biomol. Struct.* **1997**, *26*, 373–99.
(23) Tomic, J. L.; Pensalfini, A.; Head, E.; Glabe, C. G. *Neurobiol. Dis.* **2009**, *35* (3), 352–8.
(24) Nelson, R.; Sawaya, M. R.; Balbirnie, M.; Madsen, A. O.; Riekel, C.; Grothe, R.; Eisenberg, D. *Nature* **2005**, *435* (7043), 773–8.
(25) Xue, W. F.; Hellewell, A. L.; Gosal, W. S.; Homans, S. W.; Hewitt, E. W.; Radford, S. E. *J. Biol. Chem.* **2009**, *284* (49), 34272–82.
(26) Bucciantini, M.; Giannoni, E.; Chiti, F.; Baroni, F.; Formigli, L.; Zurdo, J.; Taddei, N.; Ramponi, G.; Dobson, C. M.; Stefani, M. *Nature* **2002**, *416* (6880), 507–11.

(27) Groc, L.; Lafourcade, M.; Heine, M.; Renner, M.; Racine, V.; Sibarita, J. B.; Lounis, B.; Choquet, D.; Cognet, L. *J. Neurosci.* **2007**, *27* (46), 12433–7.
(28) Calamai, M.; Specht, C. G.; Heller, J.; Alcor, D.; Machado, P.; Vannier, C.; Triller, A. *J. Neurosci.* **2009**, *29* (24), 7639–48.
(29) Saffman, P. G.; Delbruck, M. *Proc. Natl. Acad. Sci. U.S.A.* **1975**, *72* (8), 3111–3.
(30) Guigas, G.; Weiss, M. *Biophys. J.* **2006**, *91* (7), 2393–8.
(31) Ramadurai, S.; Holt, A.; Krasnikov, V.; van den Bogaart, G.; Killian, J. A.; Poolman, B. *J. Am. Chem. Soc.* **2009**, *131* (35), 12650–6.
(32) Fukuoka, H.; Sowa, Y.; Kojima, S.; Ishijima, A.; Homma, M. *J. Mol. Biol.* **2007**, *367* (3), 692–701.
(33) Renner, M.; Lacor, P. N.; Velasco, P. T.; Xu, J.; Contractor, A.; Klein, W. L.; Triller, A. *Neuron* **2010**, *66* (5), 739–54.
(34) Charrier, C.; Ehrensperger, M. V.; Dahan, M.; Levi, S.; Triller, A. *J. Neurosci.* **2006**, *26* (33), 8502–11.
(35) Andrews, N. L.; Lidke, K. A.; Pfeiffer, J. R.; Burns, A. R.; Wilson, B. S.; Oliver, J. M.; Lidke, D. S. *Nat. Cell Biol.* **2008**, *10* (8), 955–63.
(36) Frischknecht, R.; Heine, M.; Perrais, D.; Seidenbecher, C. I.; Choquet, D.; Gundelfinger, E. D. *Nat. Neurosci.* **2009**, *12* (7), 897–904.